Polymer Chemistry

Microfluidic-Supported Synthesis of Anisotropic Polyvinyl Methacrylate Nanoparticles via Interfacial Agents.

Journal:	*Polymer Chemistry*
Manuscript ID	PY-ART-12-2021-001729.R1
Article Type:	Paper
Date Submitted by the Author:	07-Mar-2022
Complete List of Authors:	Eisele, Dorthe; CUNY City College, Chemistry Visaveliya, Nikunjkumar; City College of New York, Chemistry and Biochemistry Kelestemur, Seda; Institute of Health Sciences, University of Health Sciences, Istanbul, Turkey, Biotechnology Department ; City College of the City University of New York, Chemistry and Biochemistry Khatoon, Firdaus; City College of the City University of New York Xu, Jin; City College of the City University of New York Leo, Kelvin; City College of the City University of New York St. Peter, Lauren; City College of the City University of New York Chan, Christopher; City College of the City University of New York Mikhailova, Tatiana; City College of the City University of New York Bexheti, Visar; City College of the City University of New York Kapadia, Ashni; City College of the City University of New York Carbery, William; City College of the City University of New York Ng, Kara; City College of the City University of New York Maity, Piyali; Banaras Hindu University, Physics

SCHOLARONE™
Manuscripts

Microfluidic-Supported Synthesis of Anisotropic Polyvinyl Methacrylate Nanoparticles via Interfacial Agents.

Nikunjkumar R. Visaveliya[a], Seda Kelestemur[a,b], Firdaus Khatoon[a], Jin Xu[a], Kelvin Leo[a], Lauren St. Peter[a], Christopher Chan[a], Tatiana Mikhailova[a], Visar Bexheti[a], Ashni Kapadia[a], Piyali Maity[a], William P. Carbery[a], Kara Ng[a,b], and Dorthe M. Eisele[a,c]*

For polymer particles, recent studies emphasized that the particle shape—not size—plays the dominant role in novel applications in fields ranging from nanotechnology, biomedicine, to photonics, which has intensified the quest for fabrication platforms of polymer colloids with complex non-spherical (anisotropic) shapes. Here, we developed a single-step, microfluidic-supported synthesis for anisotropic polyvinyl methacrylate (PVMA) nanoparticles (NPs) by combining the advantages of microfluidics (providing homogeneous conditions for the initial emulsification process) and bulk batch synthesis (providing inhomogenous conditions for the thermal polymerization). Specifically, we tested five interfacial agents regarding their direct impact on the NP shape (from isotropic spherical to anisotropic flower-like shapes) and their concentration-dependent impact (from 0.1 mM to 20 mM) on the NP diameter (from 200 nm to 50 nm). We employed vinyl methacrylate (VMA), a monomer offering two-polymerization active sites. With our work, we contribute to a fundamental understanding of colloidal polymerization towards predictive shapes below the critical 200-nm regime.

INTRODUCTION

Improvements in fabrication methods for polymer particles have enabled innovative applications in diverse research fields ranging from theranostics[1], targeted drug delivery[2], tissue engineering[3], to photonics[4], and beyond.[5] Similar to semiconductor or metal particles, the structure-property and structure-function relationships of polymer particles depend on the chemical composition and surface chemistry as well as on the size and shape of the particles.[6, 7] In polymer research[8-10], the importance of the particle shape[11] in structure-function relationships had been broadly overlooked. This is mainly caused by both the persistent paradigm that particle size is the dominating parameter and by the intrinsic difficulties in the fabrication of non-spherical (anisotropic) particles of soft polymeric materials. These aspects lead to the predominant use of spherical (isotropic) particles, resulting in development of solution-based fabrication platforms with a predominant focus on isotropic colloidal polymers.[12, 13] However, recent reports have emphasized that in many applications the particle shape—not size—may play the pivotal role[14, 15], which has intensified the quest for fabrication platforms of polymer colloids with complex anisotropic shapes.[16, 17]

While solution-based synthesis platforms for spherical colloidal polymers are well established[13, 18], applications utilizing anisotropic colloids[19], are restricted by limitations inherent to the overall lack of single-step synthesis platforms. In general, the shape of the polymer particles is controlled by using seeds to initiate the particle growth, that is, employing multi-step synthesis platforms.[20] In contrast to multi-step processes, single-step syntheses allow for controlled modification not only of the colloid's surface properties but also of the colloid's interior structure, essential for applications in particular in nanomedicine and biomedicine.[21, 22] Here, we address these fundamental limitations by developing a single-step emulsion polymerization[23] platform for shape-controlled anisotropic nanoscale colloids—polymer nanoparticles (NPs)—by using interfacial agents. Our microfluidic-supported synthesis approach combines the advantages of both microfluidics and batch platforms. Microfluidics[24]—a reaction technique where the manipulation of fluids takes place in channels with dimensions of tens of micrometers—allowing for precise spatio-temporal control over all synthesis parameters.[25, 26] In general, these homogenous reaction conditions within picoliter and nanoliter droplets support and enable the fabrication of colloids with highly isotropic spherical shapes.[27] On the other hand, rather inhomogeneous reaction conditions—as found, for example, in bulk batch synthesis conditions—while often leading to uncontrolled aggregation, have been viewed as a prerequisite for the creation of colloids with complex anisotropic shapes. Combining the advantages of microfluidics (for homogeneous reaction conditions) and bulk batch synthesis (for inhomogeneous reaction conditions), allows us to create anisotropic polymer NPs in a single-step process. In our microfluidic-supported approach, the initial phase—that is, emulsification of two immiscible solutions—is realized in the microreactor through employing interfacial agents, while the final phase of the polymerization takes

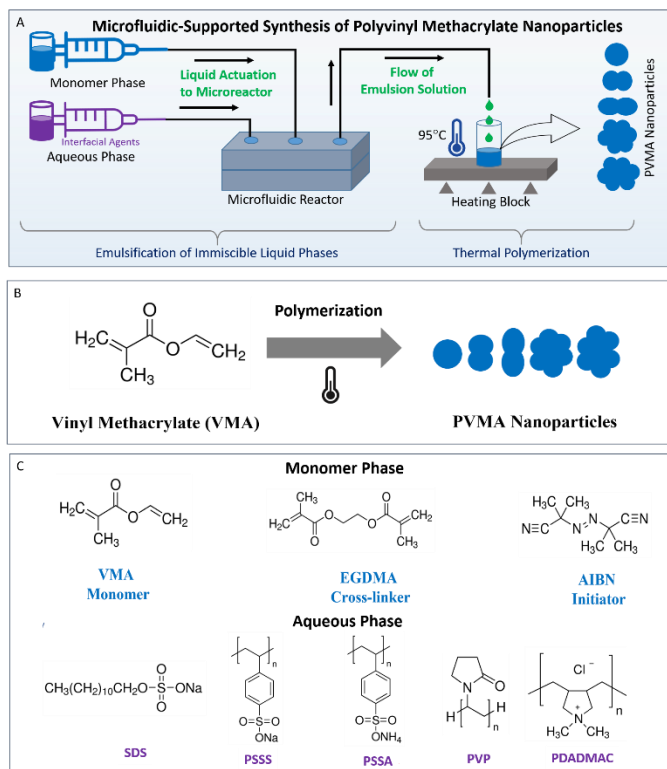a. Department of Chemistry, The City College of New York at The City University of New York, USA
b. Biotechnology Department, Institute of Health Sciences, University of Health Sciences, Istanbul, Turkey
c. PhD Program in Chemistry, Graduate Center of The City University of New York, USA
*Corresponding author: eisele@eiselegroup.com

place outside the microreactor *via* thermal polymerization at 95°C under bulk batch synthesis conditions (**Figure 1A**).

Anisotropic polymer NPs with diverse particle shapes ranging from ellipsoidal, dumbbell, rod-like, to necklace-like have been synthesized by using well-studied basic monomer systems, for example, methyl methacrylate (MMA),[28-30] a monomer with only one active polymerization site. Here, we tested the impact of the monomer as well as the interfacial agents on the NP shape and size:

Figure 1: Illustration of Microfluidic-Supported Single-Step Synthesis of Anisotropic PVMA Nanoparticles (NP) *via* Interfacial Agents. (A) Microfluidic-supported synthesis set up. The emulsification process takes place in a microreactor; two syringes, carrying monomer phase, and interfacial-agent phase, respectively, connected to the microfluidic chamber. Polymerization process completed under bulk batch conditions at the heating block. **(B)** VMA monomer, **(C)** monomer phase, and aqueous phase with interfacial agents of interest.

we employed a monomer with two active polymerization sites such as vinyl methacrylate (VMA) (**Figure 1B**) and synthesized colloidal polyvinyl methacrylate (PVMA) NPs by using various interfacial agents (**Figure 1C**). With our interfacial approach, we systematically tested five interfacial agents regarding their direct impact on the overall shape of PVMA NPs and their concentration-dependent impact (concentrations ranging from 0.1 mM to 20 mM) on the NPs dimension (diameter ranging from 200 nm to 50 nm). Specifically, anionic surfactant sodium dodecyl sulfate (SDS), anionic polyelectrolytes poly(sodium 4-styrene sulfonate) (PSSS) and poly(4-styrene sulfonic acid) ammonium salt (PSSA), non-ionic polymer polyvinylpyrrolidone (PVP), and cationic polyelectrolyte poly(diallyldimethylammonium chloride) (PDADMAC) resulted in NP shapes ranging from isotropic spherical to anisotropic flower-like NP shapes. For our polymerization reaction, we hypothesize an extended *in situ* interparticle-like colloidal assembly process during the ongoing polymerization process.

RESULTS AND DISCUSSION

Emulsion polymerization is a broadly used method to create polymeric colloidal particles.[23, 31-34] In this method, the stabilization of the organic monomer droplets dispersed in the aqueous phase, is driven by the presence of interfacial agents at the surface. Interfacial agents play therefore a crucial role during the emulsion polymerization. Not only do interfacial agents stabilize the monomer phase and form the emulsion solution, but they also initiate dynamic interfacial interaction during the growth of polymer particles that determine the size, shape, surface morphology, and the colloidal *in situ* assemblies of the polymer particles. Finally, emulsion polymerization *via* thermal initiation provides a dynamic path for the nucleation and growth of the colloidal particles. Usually, larger droplets of the monomer phase are stabilized by swollen surfactant micelles.[35] The nucleation and subsequent growth of the polymer NPs takes place when the emulsion solution reaches the specific polymerization temperature,

Our microfluidic-supported synthesis approach comprises two phases (**Figure 1**). The first phase—the monomer phase—consists of the vinyl methacrylate (VMA) monomers mixed with the cross-linker ethylene glycol dimethacrylate (EGDMA) and the thermal initiator azobisisobutyronitrile (AIBN). The second phase—the interfacial aqueous phase—consists of the different interfacial agents at various concentrations. Here, the actuation by the two syringes is key for uniformly supplying precise amounts of liquids. Then, in the cross-flow-based microfluidic reactor chamber—
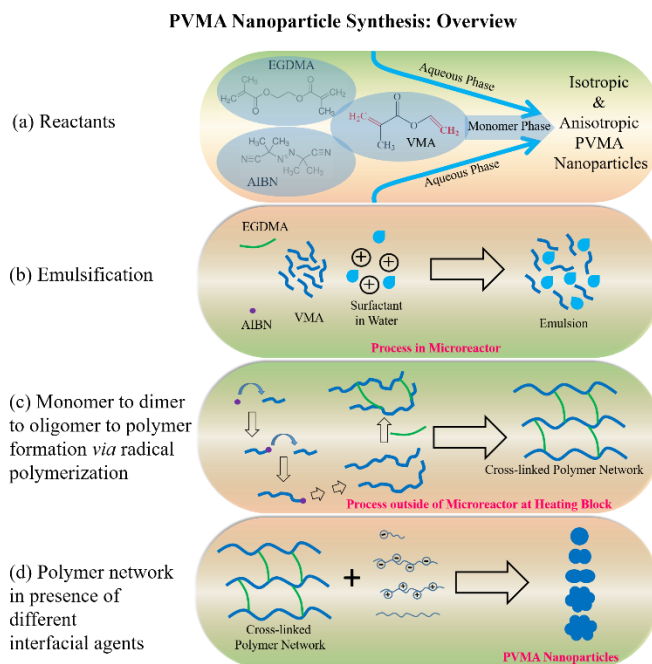

Figure 2: Proposed Emulsion Polymerization Process of PVMA NPs. The detailed description is provided in the text**.**

composed of two inlets and one outlet—the monomer droplets are formed by the emulsification of those two immiscible liquid phases.[36] The microfluidic reactor allows the formation of an emulsion of the two immiscible liquid solutions where droplets of the monomer phase are generated in the aqueous phase driven by the strong shear forces within the channels. Finally, the actual polymerization

reaction starts when the emulsion solution reaches the heating block, which is set at a constant temperature of 95°C (**Figure 1A**). A detailed description of synthesis procedures for the formation of PVMA NPs controlled by the different specific interfacial agents is provided in the **Experimental Section**. The materials characterization of the PVMA NPs *via* Zeta potential analysis and Scanning Electron Microscopy (SEM) is described in detail in the **Experimental Section**.

Previously, synthesis methods for PMMA colloids revealed that linear assembly can be realized during the polymerization process in presence of anionic polyelectrolyte PSSS resulting in shape-controlled PMMA colloids (spherical, ellipsoidal, dumbbell, and long chain-like).[28-30] Building upon these findings, we hypothesize that interfacial agents may as well play a crucial in the synthesis of shape-controlled PMMA colloids. Even though the overall mechanism for the formation of anisotropic colloidal NP is not well understood yet, it has been generally hypothesized that interfacial agents may play a role in directing the assembly of the growing NPs during the polymerization process. With this objective, we utilized a vinyl methacrylate (VMA) monomer—a monomer relatively similar to MMA[28-30] but with an additional polymerization active site, a vinyl moiety, allowing the polymer chain to grow from both ends. Furthermore, we propose that the overall shape of the PVMA NPs is governed by the interfacial agent as well as its concentration. Therefore, in our synthesis approach, we propose that the role of the interfacial agent is to control the NP's overall surface properties including its surface tension, surface functionality, and interfacial interaction.

Our proposed mechanism for the emulsion polymerization process of PVMA NPs is illustrated in **Figure 2**. Indeed, our results reveal that the shape of the obtained PVMA NPs differs depending on the used interfacial agent. For example, we obtained isotropic PVMA NPs with a spherical shape by using molecular surfactant in the aqueous phase and PVMA NPs with an elongated shape by using anionic polyelectrolytes while employing non-ionic polymer and cationic polyelectrolyte as interfacial agents resulting in diverse anisotropic PVMA NPs. In our control experiment, that is, both the emulsification process and the thermal polymerization being realized via bulk batch synthesis, we were not able to observe anisotropically shaped but only spherical PVMA NPs with inhomogeneous size distribution. On the other hand, in support of our microfluidic-supported synthesis approach for anisotropic PVMA NPs, here we provide control experiments on isotropic (spherical) PVMA NPs via molecular surfactant SDS as follows.

The Impact of Vinyl Methacrylate (VMA) Monomer

In general, the monomer unit is a building block of the polymer network. Any inherent or induced functions in the monomer can make a direct impact on the polymer network; it is known that even minor changes of the monomer can fully alter the property of the polymer network.[37, 38] A wide range of monomer units can be tailored to obtain the desired outcome/characteristics of the polymer network. Here, we selected a complex monomer analogous to MMA, i.e., vinyl methacrylate (VMA), that possesses dual polymerization active sites (two double bonds—both are eligible to grow polymer chains from both ends). As the VMA possesses dual polymerization

sites, it likely provides increased polymerization dynamics compared to MMA. Previously, the impact of VMA on RAFT polymerization under different conditions and also the impacts of various types of vinyl-based polymers, poly (vinyl acetate) and polyvinyl alcohol, on particle size and formation have been identified.[39-41]

Here, our approach is obtaining anisotropic shaped polymeric nanoparticles by emulsion polymerization. In this method, the anisotropy is achieved *via in-situ* assembly of the growing polymer nanoparticles during continuous polymerization in a single step. It is known that, in the basic model system of MMA, differently shaped nanoparticles are formed by self-assembly.[28, 30] A slight deviation in the assembly dynamics and shapes can be considered as a significant progress in a single-step formation of shape-controlled particles.

Acrylate materials, in general, are of wide interest for numerous applications.[42] Several factors need to be considered when selecting an acrylate monomer for the polymerization process; pendent hydrophobic chain length in the ester functional group of acrylate monomers, viscosity and the boiling point. VMA is not a viscous monomer to reduce the polymerization rate and it also possesses enhanced pendent hydrophobic chain length in the methacrylate monomer. Also, VMA has higher boiling point (111-112 °C) than the polymerization temperature in our semi-microfluidic method, where the colloidal formation takes place at 95°C.

The selection of monomer with multiple initiation sites can be a very promising factor for obtaining anisotropic shaped polymeric nanoparticles. By utilization of VMA, we have specifically analyzed the formation of the polymeric nanoparticles from multiple initiation sited monomer units using different interfacial agents.

Advantageously, VMA monomer can also be identified as a cross-linker due to its multiple polymerization-active sites. We have also added EGDMA as an additional cross-linker (symmetric) during the polymerization of VMA by thermal initiator AIBN, at 95°C. The utilization of cross-linker during the synthesis of polymer nanoparticles is very common (Koehler et al, Chemical Engineering Journal, 2011). It can be considered that one vinyl group of the EGDMA incorporates into the growing polymer chain, and the other vinyl group resides on a side chain pendent of the macromolecular backbone. Ideally, cross-linking is essential to achieve the topological network of the polymer and VMA is a promising monomer for this approach.

The obtained colloidal PVMA particles demonstrate that the monomer type may play a crucial role in defining the assembling pattern of particles during continuous polymerization. Despite the methodology of the polymerization being similar to the basic model system PMMA, the observed assembling pattern is significantly different under comparable reaction conditions. For instance, highly organized flower-shaped PMMA nanoparticles were obtained at all concentrations of PVP in the aqueous phase (from 10 mM to 0.1 mM, repeating unit concentrations).[30] Oppositely, flower-shaped PVMA nanoparticles were only obtained when the lower PVP concentration (0.5 mM) was used. The prevention of the assembly of growing nanoparticles to form flowers at higher PVP concentration is strongly driven by VMA, a building block of PVMA nanoparticles.

INTERFACIAL AGENTS: *Molecular Surfactant SDS*

The polymer NP's soft, flexible materials characteristic stem from their cross-linked covalent network, resulting in the energetically most favorable, spherical shape. We controlled the size of our spherically shaped PVMA NPs by using anionic molecular surfactant SDS in the aqueous phase. In general, the presence of surfactants can control the surface tension of the monomer droplets and hence the polymer NPs; higher surfactant concentration can reduce the surface tension significantly, thus smaller-sized polymer NPs can be formed.[23, 35, 43, 44]

Our approach of using molecular surfactants of different concentrations to synthesize spherical PVMA NPs is described in detail in **Supporting Information Section-1**. In general, when two immiscible liquid phases meet in presence of SDS, it is reasonable to assume that an emulsion is generated with droplets of the monomer phase stabilized by SDS molecules at the surface (so-called swollen micelles). We observed the polymerization process, which starts upon increasing the temperature of this emulsion solution, to be completed after of about 20 minutes. To control the synthesis conditions, we used syringe pumps as shown in **Figure 1A**.

Figure 3 depicts representative SEM micrographs and surface charge characteristics of our spherical PVMA NPs synthesized via various SDS concentrations. Specifically, upon application of 1 mM SDS in the aqueous phase, the diameter of the obtained spherical PVMA NPs was 75 nm ± 9.5 nm and upon application of 10 µM SDS, spherical PVMA NPs of 115 nm ± 8.9 nm in diameter were obtained. Upon further decrease of SDS concentration, application of 1 µM and 0.1 µM, spherical PVMA NPs size of 122 nm ± 12.2 nm and 163 nm ± 14 nm in diameter were obtained, respectively. We observed that the dispersion of the PVMA NP solution became denser with a continuous decrease of SDS concentration from 1 mM to 0.1 µM.

Similarly, the zeta potential analysis of the spherical PVMA NPs correlated with the applied SDS concentration: the NP's zeta potential continuously decreased with a decrease in SDS concentration. The PVMA NPs obtained *via* application of 1 mM SDS
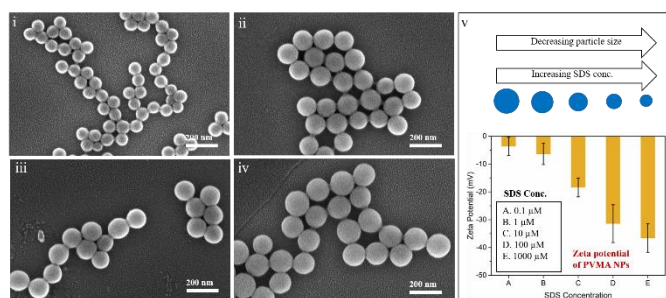

Figure 3: Spherical PVMA NPs Synthesized via Molecular Surfactant SDS. (i-iv) SEM micrographs of PVMA NPs obtained at different SDS concentrations: **(i)** 1000 µM, **(ii)** 10 µM, **(iii)** 1 µM, and **(iv)** 0.1 µM; **(v)** Zeta potential of PVMA NPs synthesized using SDS at various concentrations.

showed a zeta potential of -36.6 mV ± 5.12 mV and zeta potential of -31.4 ± 6.8 mV, -18.4 ± 3.38 mV, -6.3 mV ± 3.9 mV, and -3.6 ± 3.27 mV for PVMA NPs obtained *via* application of SDS with a concentration of 0.1 mM, 10 µM, 1 µM, and 0.1 µM, respectively (**Figure 3**).

Usually, the surfactants from micellar structures upon the surfactant's concentration being above the critical micelle concentration (CMC). The CMC of SDS is 8 mM at room temperature.[35] We have used 1 mM SDS during the synthesis of PVMA nanoparticles. Therefore, SDS concentration is below the CMC and hence it can be said that the formation of particles follows the homogeneous nucleation mechanism.[35, 41, 45]

INTERFACIAL AGENTS: *Anionic Polyelectrolytes PSSS and PSSA*

Despite their soft, flexible materials characteristic, isotropic (spherical) polymer nanoscale colloids are highly stable compared to colloids with larger dimensions or even bulk materials or colloids with non-spherical shapes. Hence, in polymer science, breaking the isotropy of spherical nanoscale colloids remains a challenge. Here, we synthesized anisotropic PVMA NPs with elongated shapes by using two, relatively similar anionic polyelectrolytes with different counterions and molecular weight: poly(4-styrenesulfonic acid) sodium salt (PSSS, 1,000,000 molecular weight, sodium ions) and poly(4-styrenesulfonic acid) ammonium salt (PSSA, 200,000 molecular weight, ammonium ions). Our approach is described in detail in **Supporting Information Section-2** and **Supporting Information Section-3**.

Figure 4i-iv and **Figure 4vi-ix** depict representative SEM micrographs and surface charge characteristics of the elongated PVMA NPs synthesized via various concentrations of PSSS and PSSA, respectively. In solution, the polymerization process might be impacted by the mobility of charged polyelectrolytes with high molecular weight, which may likely be different compared to mono-ionic surfactants with low molecular weight. Therefore, the overall mobility of PSSS and PSSA polyelectrolytes—charge and high molecular weight—impacts the colloidal growth as they are attached to the surface of growing NPs. This process might enable an assembly process to form elongated PVMA NPs. In rationalizing the cause of the NP's elongated shape, it can be imagined that spheres assemble assisted by long-chained charged polyelectrolytes with the polyelectrolyte chain enable to move flexibly, allowing the formation of hydrophobic PVMA NPs in a linear direction.[28-30] Application of higher PSSS concentration (20 mM, repeating unit concentration) resulted in ellipsoidal-like shaped PVMA NPs as shown in **Figure 4i**.

Interestingly, with continuously decreasing PSSS concentration from 10 mM to 2.5 mM and 1 mM, the PVMA NPs became larger and more elongated (**Figure 4ii-iv**). Similar to our above results on using molecular surfactants as interfacial agents, increased protection of NP surface can be realized upon increased polyelectrolyte (PSSS) concentration. Specifically, at higher PSSS concentration (20 mM), the size and overall assembly pattern are decreased of the elongated PVMA NPs (**Figure 4i**). When PSSS concentration has been further decreased down to 10 mM (**Figure 4ii**), the assembly pattern further increased with a slight increase of overall size of the PVMA NPs compared to the NPs obtained during application of 20 mM PSSS concentration. Upon further decrease of PSSS concentration, we observed irregularity in
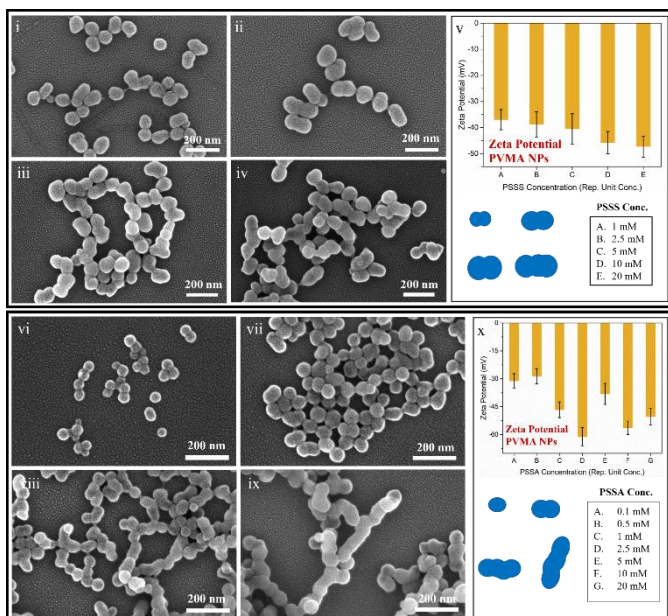
Figure 4: Elongated PVMA NPs Synthesized via Anionic Polyelectrolytes PSSS and PSSA. **(i-iv)** SEM micrographs of PVMA NPs obtained at different PSSS repeating-unit concentrations: **(i)** 20 mM, **(ii)** 10 mM, **(iii)** 2.5 mM, and **(iv)** 1 mM. **(v)** Zeta potential of PVMA NPs obtained during the application of PSSS in an aqueous phase at tunable concentration. **(vi-ix)** SEM micrographs of the PVMA NPs obtained at different PSSA repeating-unit concentrations in aqueous phase: **(vi)** 10 mM, **(vii)** 2.5 mM, **(viii)** 0.5 mM, and **(ix)** 0.1 mM. **(x)** Zeta potential of PVMA NPs synthesized using PSSA at various concentrations.

the assembly pattern towards the linear direction, as shown in (**Figure 4iii-iv**).

As interfacial agents such as polyelectrolyte PSSS are assumed to impact the overall assembly behavior, the surface charge of the PVMA NPs may change upon the use of different PSSS concentrations. As expected, the zeta potential values were found to decrease with a decrease in PSSS concentrations in the aqueous phase. In the case of 20 mM PSSS concentration, we observed a zeta potential of PVMA NPs of -47.3 mV ± 4.03 mV (high value in negative direction likely because of the anionic polyelectrolyte PSSS). In addition, the zeta potential value of PVMA NPs was obtained -38.8 mV ± 4.83 mV, -40.5 mV ± 5.79 mV, and -45.8 mV ± 4.26 mV, during the application of 2.5 mM, 5 mM, and 10 mM, PSSS concentrations, respectively (**Figure 4v**).

We tested a second anionic polyelectrolyte, that is, PSSA (200,000 molecular weight) regarding its impact on PVMA NP formation. Interestingly, despite both PSSA and PSSS being alike anionic polyelectrolytes, the obtained nanoparticles are different in terms of assembling pattern. We observed a similar type of linear assembly pattern but a slightly different length for PSSA compared to PSSS in the aqueous phase. As the counter ions of the PSSA and PSSS differ—cationic ammonium ions and sodium ions, respectively—it might be possible that during the dynamic polymerization reaction, both the radical-driven growing polymer chain and freely moving counter ions interact with one another. This interaction may impact the assembling events of the growing NPs. Hence, the different counter ions of PSSS and PSSA may play a major role in directing the NP assembly, however, the detailed mechanism is still unclear as it requires further characterization *via* XPS analysis and related techniques, which is beyond the current scope of this report.

We estimate that the PSSS (or PSSA) likely covers only a few nanometres (less than 10 nm of surface thickness) whereas about 90% of the NP volume may stem from PVMA. This estimation takes into account that the PSSS (or PSSA) volume (weight) is less than 0.5% of the VMA monomer volume (weight), so it is reasonable to assume that the NPs are filled with PVMA. However, to determine the relative uptake of PSSS (or PSSA) and PVMA in the PVMA NPs requires further chemical characterizations that are beyond the scope of this work.

Figure 4vi-ix depicts representative SEM micrographs and surface charge characteristics of our elongated PVMA NPs synthesized via PSSA at various concentrations. Interestingly, the zeta potential (negative likely due to anionic characteristics of the PSSA) is not consistent with the concentration of PSSA as shown in **Figure 4x**. This inconsistency in the zeta potential value may be caused by the irregular assembly pattern of the PVMA NPs that is driven by the functional monomer system VMA.

INTERFACIAL AGENTS: *Non-ionic Polymer PVP*

As a non-ionic interfacial agent for PVMA NPs synthesis, we employed polymer polyvinylpyrrolidone (PVP). Surprisingly, in contrast to our results described above obtained at higher concentrations SDS, PSSS or PSSA, at higher concentrations of PVP, we did not observe assembly pattern of PVMA NPs. Instead, assembly patterns were observed when the concentration of PVP was continuously decreased. We observed flower-type shape PVMA NPs at very low PVP concentrations.
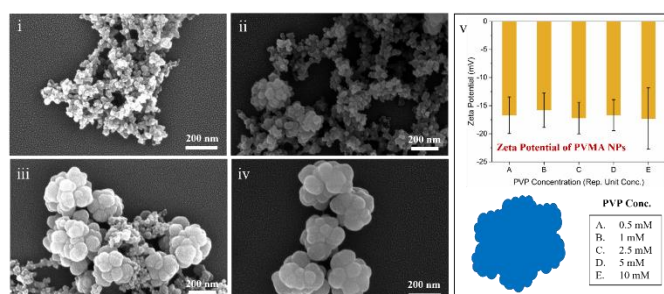

Figure 5: Flower-like Shaped PVMA NPs Synthesized *via* Non-ionic Polymer PVP. While at higher PVP concentration in the aqueous phase, no systematic assembly was observed, at lower PVP concentrations, flower-like shaped assemblies were observed. **(i-iv)** SEM micrographs of PVMA NPs obtained at different PVP repeating-unit concentrations: **(i)** 10 mM, **(ii)** 2.5 mM, **(iii)** 1 mM, and **(iv)** 0.5 mM. **(v)** Zeta potential of PVMA NPs synthesized using PVP at various concentrations.
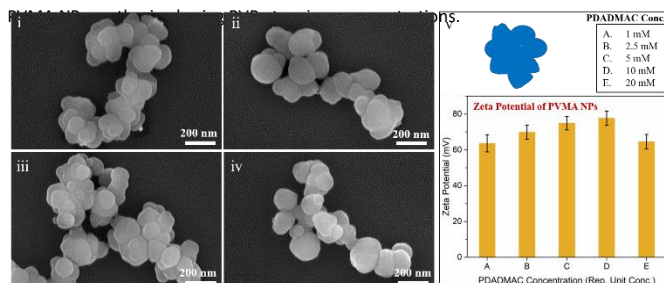

Figure 6. PVMA NPs Synthesized via Cationic Polyelectrolyte PDADMAC. (i-iv) SEM micrographs of PVMA NPs obtained at different PVP repeating-unit concentrations: (i) 20 mM, **(ii)** 10 mM, **(iii)** 5 mM, and **(iv)** 1 mM. Scale bar for all SEM images 200 nm. **(v)** Zeta potential of PVMA NPs synthesized using PDADMAC at various concentrations.

Specifically, at a PVP concentration of 10 Mm (repeating unit concentration) no assembly pattern of the PVMA NPs were

found (**Figure 5i**) but we found an increasing tendency for assembly patterns of PVMA NPs when the concentration of PVP decreased gradually from 2.5 mM and 1 mM, as shown in **Figures 5ii** and **5iii**, respectively. Moreover, a flower-type-like shape assembly pattern was obtained when 0.5 mM PVP concentration was applied in the aqueous phase (**Figure 5iv**). The relatively unchanged zeta potential (about -17 mV) can be explained by the non-ionic character of PVP (**Figure 5v**). Overall, taking into consideration that PVP is neutral, as are VMA and EGDMA, and the zeta potential of -17 mV is a relatively high negative charge. The result can be explained by the PVP attached to the PVMA NP's surface, their chain is exposed to the aqueous solution, likely resulting in keto-enol transition through enolization. Our approach is described in detail in **Supporting Information Section-4**.

The assembly of PVMA nanoparticles, grown under the influence of PVP as an interfacial agent, is considered as multiple aggregation phases during continuous polymerization. Due to the functional VMA monomer, the concentration of PVP is crucial here, unlike the case of the MMA monomer.[30] At higher PVP concentration, it is believed that the surface is strongly covered by PVP until all the monomers are consumed and the aggregation (in-situ assembly) is prevented. When the concentration of the PVP is lowered down to 1 mM (repeating unit concentration), the assembly started to form as the surface is partially covered with PVP and hence hydrophobic PVMA particles are formed. Furthermore, overall assembling nanoparticles were obtained at 0.5 mM (repeating unit PVP concentration) because of the quick hydrophobic aggregation. These results suggested that the monomer system plays a critical role in deriving an assembly pattern that can impact the shapes of particles under certain reaction conditions.

INTERFACIAL AGENTS: *Cationic Polyelectrolyte PDADMAC*

Finally, as a cationic interfacial agent for PVMA NPs synthesis, we employed polyelectrolyte polydiallyldimethylammonium chloride (PDADMAC, molecular weight 200,000-350,000). During the application of PDADMAC, even though assembly patterns of PVMA NPs were observed, the obtained NP shapes did *not* show regular structural characteristics. Similar to spherically-shaped PVMA NPs obtained with SDS, polymerization starts upon temperature increase of the PDADMAC emulsion solution (heating block, as shown in **Figure 1**). The assembly pattern of PVMA NPs is irregular at all concentrations ranging from 1 mM to 20 mM (repeating unit concentration) as shown in **Figure 6i-iv**. Due to the PDADMAC, the surface charge of the NPs is cationic. The zeta potential value is high and obtained in the range of about +70 mV as shown in **Figure 6v**. Our approach is described in detail in **Supporting Information Section-5.**

CONCLUSION

We developed a microfluidic-supported synthesis platform for anisotropic polyvinyl methacrylate (PVMA) nanoparticles (NPs) *via* interfacial agents. By employing a molecular surfactant, anionic and cationic polyelectrolytes, and a non-ionic polymer as our interfacial agents of interest, our study provides further evidence that both the type of monomer as well as the interfacial agents play a critical role in controlling the anisotropic assembly pattern of colloidal polymer PVMA NPs, in particular. Specifically, we found that the molecular surfactant SDS is crucial for the formation of spherically shaped PVMA NPs while the anionic polyelectrolytes PSSS and PSSA result in the formation of PVMA NP with elongated shapes. Beyond charged polyelectrolytes, using non-ionic polymer PVP, we found that using a higher PVP concentration did not result in assemblies with regular structural characteristics, but using a lower PVP concentration supported the formation of flower-like shaped assembly patterns of PVMA NPs. Furthermore, we employed cationic polyelectrolyte PDADMAC as an interfacial agent for the synthesis of PVMA NPs and observed irregularly shaped assembly formation. Overall, with our work, we provide a general framework allowing for fundamental investigations on colloidal polymerization towards predictive shapes below the critical 200-nm regime.

EXPERIMENTAL SECTION

Microreactor Design and Arrangement

A microreactor was used for the control of liquid flow and consists of two walls. The silicon hole-plate is placed inside the chamber walls, has been fabricated via a lithographic method as described previously.[36] One chamber wall (base) has a channel whose internal diameter is 0.8 mm. Another chamber wall (cap) has a space for accommodating the lithographically prepared silicon chip and also has three valves (two inlets and one outlet). Once the silicon hole-plate is placed inside the chamber, it is packed with screws and made ready for connectors for actuating the liquid solutions. The full detail and fabrication process of the microreactor has been previously described in detail.[36] A photo as well as schematic illustration of the microreactor is provided in the Supporting Information.

Synthesis of Polyvinylmethacrylate (PVMA) Nanoparticles.
Polyvinylmethacrylate (PVMA) nanoparticles of different sizes in the case of isotropic (spherical) nanoparticles and anisotropy were prepared *via* semi-microfluidic syntheses. The general process of the formation of PVMA nanoparticles is emulsion polymerization. First, two immiscible liquid phases were prepared separately for emulsification: the interfacial aqueous phase—consists of the different interfacial agents at various concentrations—and the monomer phase—consists of the vinyl methacrylate (VMA) monomers mixed with the cross-linker ethylene glycol dimethacrylate (EGDMA) and the thermal initiator azobisisobutyronitrile (AIBN)).

The interfacial aqueous phase contains various interfacial agents of different concentrations. In our experiments, we used five different interfacial agents: (i) Poly(sodium 4-styrene sulfonate) (PSSS) (average Mw ~1,000,000, powder) (Sigma-Aldrich), (ii) Polyvinylpyrrolidone (PVP) (average molecular weight 40,000) (Sigma-Aldrich), (iii) Poly(4-styrene sulfonic acid) ammonium salt solution (PSSA) (Mw ~200,000, 30 wt. % in H_2O) (Sigma-Aldrich), (iv) Sodium dodecyl sulfate (SDS) (ACS reagent, ≥99.0%, Sigma-Aldrich), (v) Poly(diallyldimethylammonium chloride) solution (PDADMAC) (average Mw 200,000-350,000 (medium molecular weight), 20 wt. % in H_2O) (Sigma-Aldrich). Five different concentrations for PSSS have been used: (A) 20 mM (repeating unit concentration), (B) 10 mM

(repeating unit concentration), (C) 5 mM (repeating unit concentration), (D) 2.5 mM (repeating unit concentration), (E) 1 mM (repeating unit concentration). Similarly, five different concentrations of PVP have been used for different experiments: (A) 10 mM (repeating unit concentration), (B) 5 mM (repeating unit concentration), (C) 2.5 mM (repeating unit concentration), (D) 1 mM (repeating unit concentration), (E) 0.5 mM (repeating unit concentration). Likewise, seven different concentrations of PSSA have been used: (A) 20 mM (repeating unit concentration), (B) 10 mM (repeating unit concentration), (C) 5 mM (repeating unit concentration), (D) 2.5 mM (repeating unit concentration), (E) 1 mM (repeating unit concentration), (F) 0.5 mM (repeating unit concentration), (G) 0.1 mM (repeating unit concentration). In another experiments, five different concentrations of SDS has been used: (A) 1000 μM, (B) 100 μM, (C) 10 μM, (D) 1 μM, and (E) 0.1 μM. Lastly, five different concentrations of PDADMAC have been used: (A) 20 mM (repeating unit concentration), (B) 10 mM (repeating unit concentration), (C) 5 mM (repeating unit concentration), (D) 2.5 mM (repeating unit concentration), (E) 1 mM (repeating unit concentration). The monomer phase was made up of a mixture of monomer, cross-linker, and thermal initiator. For making the 1 mL of monomer phase solution, 4 μg Azobisisobutyronitrile (AIBN) (98%, Sigma-Aldrich) and 10 μL Ethylene glycol dimethacrylate (EGDMA) (98%, Sigma-Aldrich) has been dissolved to 990 μL of vinyl methacrylate (VMA) (98%, Sigma-Aldrich).

The solution of the monomer phase has been filled in the 3 mL syringe and the solution of the aqueous phase has been filled in the 10 mL sized syringe. Both syringes were applied to two different syringe pumps (New Era Pump System Inc., syringepump.com). The flow rate ratio of the monomer phase was set to 80 μL/min and for the aqueous phase to 1200 μL/min. The tubing internal diameter is 0.8 mm. Both syringes were attached to the microfluidic chamber (**Figure 1A**): the first two valves are inlet; cross-flow T-junction; the third valve is an outlet.

As schematically illustrated in **Figure 1A**, the emulsion has been collected in a small vial (1.5 ml size) which was arranged at the heating block at the polymerization temperature of 95°C (heating block temperature). The polymerization reaction kept running in the vial for 20 minutes under moderate stirring conditions (no stirrer, but gentle shaking by hand so that the sensitive assembly process is not disturbed). Once the polymerization process is finished, the vial has been removed from the heating block and allowed to cool down to room temperature. Afterward, dispersed polymer nanoparticles (polymerization product) washed with double distilled water by two-cycle of centrifugation each with 11,000 RPM for 12 minutes. Once the nanoparticles are purified, their characterization in the scanning electron microscopy and zeta sizer has been performed. In general, in this two-phase process combining microfluidics and batch, the polymerization process is slower for higher surfactant concentration, for example, during the application of 1 mM SDS, the polymerization reaction time was about 12-15 minutes but during the application of 0.001 mM SDS, the reaction time was only 6-8 minutes.

In general, monomers and cross-linker were used as received (pure solutions, not dissolve in any solvent) and were measured in volume.

Scanning Electron Microscopy (SEM) Characterization. For getting scanning electron microscope (SEM) images, obtained polyvinylmethacrylate (PVMA) nanoparticles via semi-microfluidic synthesis were washed with double distilled water by applying two cycles of centrifugation (11,000 RPM, 12 minutes). The supernatant has been discarded and nanoparticles were re-dispersed in double-distilled water. For preparing the SEM chip, 10 μL of nanoparticles dispersion was added to the 100 μL (dilution). Afterward, a tiny drop of 2 μL of diluted NPs solution has been deposited on the 500 nm thick washed silicon chip. A chip is kept on the glass slide at the benchtop to allow evaporation of water naturally. Once the water is evaporated and the NPs adsorbed to the surface, a water flow has been applied gently on the silicon chip to remove the non-adsorbed NPs. Afterward, gold sputtering (thickness: 2.7 nm) has been applied to the silicon chip by Leica EM ACE600 Coater. After sputtering, the silicon chip is fixed to the holder with conductive tape. The chip holder is then brought to the SEM chamber and a vacuum has been created for SEM operation. An FEI Helios Nanolab 660 FIB-SEM instrument has been used for the imaging of the polymer NPs. Imaging was taken at 5 KV voltage and 25 PA current at multiple magnifications.

Zeta Potential Characterization. The Zeta potential of the PVMA nanoparticles was measured by the Malvern Zetasizer instrument (Zetasizer Nano Series: Nano ZS). Initially, the centrifuged particles were re-dispersed in double-distilled water. 50 μL of nanoparticles dispersion has been diluted to the 1 mL double distilled water. Afterward, 1 mL diluted NPs dispersion has been filled to the zeta potential measurement cell (Malvern: DTS1070) for measuring its zeta potential. Zeta potential has been measured at room temperature with 1/100 runs for three repeated measurement cycles. 27 different samples of the NPs were measured in the zeta sizer. The zeta potential value has been obtained with their standard deviation. The results were organized in the cumulative graphs as shown in the main manuscript.

AUTHOR INFORMATION

Corresponding Author

*Corresponding author: eisele@eiselegroup.com

CONFLICTS OF INTEREST

The authors declare no conflict of interest.

AUTHORS CONTRIBUTION

D.M.E. directed the project; N.R.V. designed experiments; J.X., F.K., K.L., L.S.P., and T.M. supported in the experimental setup and syntheses of polymer nanoparticles; J.X., C.C., and V.B. supported in purification and characterization of polymer nanoparticles; F.K. and L.S.P. supported in SEM imaging; J.X., A.K., L.S.P., K.L., and F.K. supported in zeta potential measurements; P.M., S.K., W.P.C., and K.N. provided data interpretation and fruitful discussions during the preparation of the manuscript; D.M.E., S.K., P.M., and N.R.V. co-wrote the manuscript with inputs from all co-authors.

REFERENCES

1. M. Elsabahy, G. S. Heo, S.-M. Lim, G. Sun and K. L. Wooley, *Chemical Reviews*, 2015, **115**, 10967-11011.

2. B. Fortuni, T. Inose, M. Ricci, Y. Fujita, I. Van Zundert, A. Masuhara, E. Fron, H. Mizuno, L. Latterini, S. Rocha and H. Uji-i, *Scientific Reports*, 2019, **9**, 2666.

3. I. O. Smith, X. H. Liu, L. A. Smith and P. X. Ma, *WIREs Nanomedicine and Nanobiotechnology*, 2009, **1**, 226-236.

4. G.-H. Lee, H. Moon, H. Kim, G. H. Lee, W. Kwon, S. Yoo, D. Myung, S. H. Yun, Z. Bao and S. K. Hahn, *Nature Reviews Materials*, 2020, **5**, 149-165.

5. M. J. Monteiro and M. F. Cunningham, *Biomacromolecules*, 2020, **21**, 4377-4378.

6. D. Walsh and D. Guironnet, *Proceedings of the National Academy of Sciences*, 2019, **116**, 1538 - 1542.

7. A. Albanese, P. S. Tang and W. C. W. Chan, *Annual Review of Biomedical Engineering*, 2012, **14**, 1-16.

8. M. W. Lampley and E. Harth, *ACS Macro Letters*, 2018, **7**, 745-750.

9. Y. Tian, M. V. Kuzimenkova, M. Xie, M. Meyer, P.-O. Larsson and I. G. Scheblykin, *NPG Asia Materials*, 2014, **6**, e134-e134.

10. B. Zhao, M. A. C. Serrano, J. Gao, J. Zhuang, R. W. Vachet and S. Thayumanavan, *Polymer Chemistry*, 2018, **9**, 1066-1071.

11. S. Sacanna and D. J. Pine, *Current Opinion in Colloid & Interface Science*, 2011, **16**, 96-105.

12. J. W. Hickey, J. L. Santos, J.-M. Williford and H.-Q. Mao, *Journal of Controlled Release*, 2015, **219**, 536-547.

13. J. P. Rao and K. E. Geckeler, *Progress in Polymer Science*, 2011, **36**, 887-913.

14. J. A. Champion and S. Mitragotri, *Proceedings of the National Academy of Sciences of the United States of America*, 2006, **103**, 4930-4934.

15. D. M. Richards and R. G. Endres, *Proceedings of the National Academy of Sciences*, 2016, **113**, 6113-6118.

16. K. V. Edmond, T. W. P. Jacobson, J. S. Oh, G.-R. Yi, A. D. Hollingsworth, S. Sacanna and D. J. Pine, *Soft Matter*, 2021, **17**, 6176-6181.

17. M. He, J. P. Gales, X. Shen, M. J. Kim and D. J. Pine, *Langmuir*, 2021, **37**, 7246-7253.

18. K. Nakabayashi, M. Kojima, S. Inagi, Y. Hirai and M. Atobe, *ACS Macro Letters*, 2013, **2**, 482-484.

19. Z. Gong, T. Hueckel, G.-R. Yi and S. Sacanna, *Nature*, 2017, **550**, 234-238.

20. J. G. Park, J. D. Forster and E. R. Dufresne, *Journal of the American Chemical Society*, 2010, **132**, 5960-+.

21. N. R. Visaveliya, C. W. Leishman, K. Ng, N. Yehya, N. Tobar, D. M. Eisele and J. M. Köhler, *Advanced Materials Interfaces*, 2017, **4**, 1700929.

22. A. Zielińska, F. Carreiró, A. M. Oliveira, A. Neves, B. Pires, D. N. Venkatesh, A. Durazzo, M. Lucarini, P. Eder, A. M. Silva, A. Santini and E. B. Souto, *Molecules*, 2020, **25**, 3731.

23. P. A. Lovell and F. J. Schork, *Biomacromolecules*, 2020, **21**, 4396-4441.

24. G. M. Whitesides, *Nature*, 2006, **442**, 368-373.

25. D. Dendukuri and P. S. Doyle, *Advanced Materials*, 2009, **21**, 4071-4086.

26. A. B. Theberge, F. Courtois, Y. Schaerli, M. Fischlechner, C. Abell, F. Hollfelder and W. T. S. Huck, *Angewandte Chemie-International Edition*, 2010, **49**, 5846-5868.

27. M. H. Reis, F. A. Leibfarth and L. M. Pitet, *ACS Macro Letters*, 2020, **9**, 123-133.

28. N. Visaveliya and J. M. Kohler, *Acs Applied Materials & Interfaces*, 2014, **6**, 11254-11264.

29. N. Visaveliya and J. M. Kohler, *Macromolecular Chemistry and Physics*, 2015, **216**, 1212-1219.

30. N. Visaveliya and J. M. Köhler, *Langmuir*, 2014, **30**, 12180-12189.

31. S. Gao, S. Song, J. Wang, S. Mei, J. Yuan, G. Liu and M. Pan, *Colloids and Surfaces A: Physicochemical and Engineering Aspects*, 2019, **577**, 360-369.

32. A. R. Goodall, M. C. Wilkinson and J. Hearn, *Journal of Polymer Science: Polymer Chemistry Edition*, 1977, **15**, 2193-2218.

33. E. B. Mock and C. F. Zukoski, *Langmuir*, 2010, **26**, 13747-13750.

34. J. W. Vanderhoff, *Journal of Polymer Science: Polymer Symposia*, 1985, **72**, 161-198.

35. C. S. Chern, *Progress in Polymer Science*, 2006, **31**, 443-486.

36. J. M. Koehler, F. Moeller, S. Schneider, P. M. Guenther, A. Albrecht and G. A. Gross, *Chemical Engineering Journal*, 2011, **167**, 688-693.

37.   T. Fujiyabu, Y. Yoshikawa, U.-i. Chung and T. Sakai, *Science and Technology of Advanced Materials*, 2019, **20**, 608-621.

38.   A. J. Guenthner, K. R. Lamison, V. Vij, J. T. Reams, G. R. Yandek and J. M. Mabry, *Macromolecules*, 2012, **45**, 211-220.

39.   M. Akiyama, K. Yoshida and H. Mori, *Polymer*, 2014, **55**, 813-823.

40.   H.-T. Hsieh, H.-M. Chang, W.-J. Lin, Y.-T. Hsu and F.-D. Mai, *Scientific Reports*, 2017, **7**, 9531.

41.   W. J. Priest, *The Journal of Physical Chemistry*, 1952, **56**, 1077-1082.

42.   Y. Bao, J. Ma, X. Zhang and C. Shi, *Journal of Materials Science*, 2015, **50**, 6839-6863.

43.   V. B. Fainerman, E. V. Aksenenko, A. V. Makievski, M. V. Nikolenko, A. Javadi, E. Schneck and R. Miller, *Langmuir*, 2019, **35**, 15214-15220.

44.   M. J. Qazi, S. J. Schlegel, E. H. G. Backus, M. Bonn, D. Bonn and N. Shahidzadeh, *Langmuir*, 2020, **36**, 7956-7964.

45.   R. M. Fitch, *British Polymer Journal*, 1973, **5**, 467-483.